中國機械工程學刊第四十四卷第三期第 273~285 頁(民國一百一十二年)
Journal of the Chinese Society of Mechanical Engineers, Vol.44, No.3, pp273~285 (2023)

Perforation and Failure-Tolerant Mechanism of AA/CFRP Stack Sheets Under Quasi-Static Loading Conditions

Zhaobing Liu *, Yaoyao Yu ** and Kerui Peng ***

Keywords：AA/CFRP stack sheets, Perforation, Deformation mechanism, Energy absorption.

ABSTRACT

Loading conditions have a strong influence on the mechanical performance of Aluminum Alloy(AA)/Carbon Fiber Reinforced Plastic (CFRP) stack sheets. However, the understanding of its deformation behavior under perforation loading is still limited. The aim of this study is to investigate the perforation and failure tolerance mechanism of AA/CFRP stack sheets when subjected to quasi-static perforation loads. The effects of factors such as layer arrangement, tool indenter size, and mechanical properties of each layer on the mechanical performance of AA/CFRP stack sheets were analyzed by analytical and/or experimental methods under quasi-static penetration loading conditions. During the quasi-static penetration loading, layer arrangement is the most dominating factor affecting the penetration deformation behaviors. If the CFRP layer faces the tool indenter, failure in the AA metal layer could be advanced to some extent. A dishing deformation is observed first. Then, tensile tearing at the center of the sheet dominates the failure mode. When the AA layer faces the tool indenter, the mechanical behavior of the stack sheet strongly depends on the failure mode of the metal plate. It is noting that the metal layer fails in a very similar way to the monolithic metal sheet. Nevertheless, the CFRP sheet was able to resist more bending deformation of the metal layer, thereby increasing energy dissipation. Furthermore, increasing the thickness of the CFRP sheet could postpone the fracture of the metal layer. In addition, the damage pattern of AA metal layer under 5mm indenter diameter is a circular shape regardless of monolithic or stack sheets, while the damage pattern of AA metal layer in the other two diameter cases shows a petaloid shape. This is mainly because a smaller tool contact surface during perforation more easily experiences from elastic bending to a whole circumferential tensile tearing. By contrast, a larger tool contact surface leads to bi-axial even multi-axial tensile tearing. Moreover, the developed analytical mode can predict the variation trends of perforation energy correctly. Our findings show that applying a metal layer to the CFRP sheet can provide a practical method to enhance the mechanical performance of existing CFRP materials.

Paper Received November, 2022. Revised January, 2023. Accepted March, 2023. Author for Correspondence: Zhaobing Liu

* *Associate Professor, School of Mechanical and Electrical Engineering, Wuhan University of Technology，Wuhan 430070, China.*

** *Graduate Student, School of Mechanical and Electrical Engineering, Wuhan University of Technology，Wuhan 430070, China.*

*** *Graduate Student, School of Mechanical and Electrical Engineering, Wuhan University of Technology，Wuhan 430070, China.*

INTRODUCTION

Carbon fiber reinforced plastics (CFRP) have led to the increasing use in many industrial sectors, such as automobile, civil, aircraft and aerospace applications, due to the high performance, light weight, specific strength and stiffness characteristics (Smith, 1990). In recent years, multi-material stacks obtained by combining two or more layers of CFRP and metal have received much attention because of their importance in the manufacture of structures subjected to very high mechanical service loads, which are often difficult or impossible to obtain with a single material (Kuo et al., 2017; Luo et al., 2015). Specifically, aluminum alloy (AA)/CFRP stack sheet is preferable in aircraft structures for weight reduction (Xia and Mahdavian, 2005; Zitoune et al., 2012; Zitoune et al., 2010). In order to take full advantage of AA/CFRP stack sheets, it is necessary to understand the deformation behavior of such materials under quasi-static conditions.

Literature review reveals that great efforts have been made to investigate the different deformation behaviors of monolithic sheets or multi-material stack composites (e.g. CFRP/AA sheets) under impact and quasi-static loading and their effects on the perforation resistance. For example, for an AA sheet, Wierzbicki (1999) investigated the petalling induced failure mode of monolithic metal plates under impact and explosive loading. An analytical method was proposed to provide a good qualitative and quantitative analysis well validated by experimental data. Simonsen and Lauridsen (2000) studied the mechanics of lateral penetration of a rigid spherical tool into a monolithic metal sheet through analytical theory, numerical analysis, and experimental validation. They found that the indentation to ductile fracture and the energy absorption were sensitive to several process parameters such as plate geometry, loading position and tool geometry. Based on the energy conservation principle, Chen et al. (2007) established a new analytical model to predict the residual velocities of the tool with a hemispherical shape nose for the penetration of thin steel plates at low velocities. They pointed out that the analytical predictions agreed well with the experimental results. Schwab et al. (2016) investigated the damage that occurs in CFRP monolithic sheets under compression and impact loading, such as matrix crack formation, delamination and fiber fracture. Mohagheghian et al. (2015, 2017a, 2017b, 2016) conducted a series of experiments to systematically study the penetration kinetics of monolithic polymer and metal plates under static and impact loading while considering the variation of the tip shape. They concluded that the perforation of blunt-tipped and hemispherical tips is more sensitive to local deformation and that the optimal ratio of polymer to metal thickness maximizes the perforation resistance of this bilayer structure relative to a single metal sheet of the same mass. Yuan et al. (2021) investigated the mechanical behavior of CFRP beams and square plates under transverse local loads, including quasi-static indentation loads and impact loads. Experimental results indicate that CFRP specimens of the beam shape have higher perforation resistance as well as more damage patterns than that of the square shape. The effect of matrix shear strength on the ballistic response of flat-headed projectile simply supported CFRP beams was investigated by quasi-static indentation tests and quasi-static shear tests on rigid back support of carbon fiber fabric beams by Yu et al. (2017). They concluded that CFRP laminates have excellent structural properties under quasi-static loading conditions, but weaker impact resistance in dynamic environments than composites made from flexible fibers. Xu et al. (2017) investigated the scaling effect on the perforation resistance of plain weave carbon fiber composite laminates under quasi-static and impact loading conditions. It was shown that the elastic response of the composite beams and plates follows a scaling law, whereas the maximum load at failure generally decreases with increasing scale size.

In contrast to the penetration mechanics of monolithic panels, the ability of metal surface layers to protect CFRP panels against perforation was explored by Yu et al. (2018). The results showed that the perforation mechanism of the CFRP layer was not affected by either the presence of the metal layer or the choice of loading rate (i.e., quasi-static versus ballistic), but by adding a protective metal layer, the loading area in the CFRP layer increased, thereby increasing the resistance of the CFRP layer to perforation. Li et al. (2021) proposed and designed a novel fiber-metal hybrid laminate (FM-HLC). The failure results of FM-HLC under quasi-static tensile, three-point bending, and projectile impact tests, have showed that the proposed design strategy has significant potential to address metal-composite interface (MCI) failure in fiber-metal composites. Through analytical and experimental analyses, Liu and Chen et al. (2020) investigated the deformation mechanism and damage tolerant properties of a novel weakly adherent polymer-coated sheet metal laminate (PSML) under quasi-static penetration and more complex dynamic incremental deformation loads. The results suggest that coating PA on weakly bonded metal sheets may provide a practical solution for improving the mechanical properties of existing metallic materials. Experimental and numerical analysis of quasi-static perforation of metal fiber laminates (FML) at high temperatures concluded in (Chow et al., 2021) that most of the energy dissipation is caused by aluminum plastic deformation and only a small fraction is caused by adhesive delamination, FRP fiber fracture and matrix cracking. From the above comments, there is a growing interest in studying the properties of composites with different structures under quasi-static loading (Yeganeh et al., 2016; Anbazhagan et al., 2022; Garrido et al., 2021; Garrido et al., 2021; Linforth et al., 2021; Javanshour et al., 2021). The perforation characteristics and damage-resistant mechanism needs to be further investigated.

In this work, we propose a stack material that is composed of CFRP and AA metal sheets. Given such material, perforation characteristics have been comprehensively investigated through analytical and experimental methods when quasi-static loading is applied by hemispherical-shape tool indenter. The mechanical responses, especially failure-resistant capability, are explored in terms of the effects of material layer arrangements, tool indenter sizes, and mechanical properties of each layer compared with monolithic materials.

The rest of this paper is organized as follows.

Section 2 introduces the composition of the materials and experimental methodology. Mechanical responses including deformation mechanism and failure modes for quasi-static perforation are presented and discussed in Section 3. Conclusions are given in the last section.

MATERIALS AND EXPERIMENTS

AA/CFRP stack sheets

The AA/CFRP stack sheet consists of aluminum alloy (AA) 1060-H24 metal and CFRP (Carbon fiber reinforced plastic-PA6). The proposed AA/CFRP stack sheet can provide a typical and convenient material model system for studying the mechanical response of bilayer materials. To characterize the materials, the tensile stress-strain curves for AA and CFRP sheets with a thickness of 1 mm are obtained in Figure 1. In addition, the detailed information of stack materials is presented in Table 1.

We made AA/CFRP laminated sheets by stacking CFRP sheets and AA1060-H24 sheets of the same dimensions, see Figure 2. The AA and CFRP sheets were cut into small pieces with dimensions of 100 mm × 100 mm for use. It is noting that in this investigation, we only consider the effect of CFRP thickness variation on the perforation mechanism of bilayer sheets under quasi-static loading conditions, so the thickness of AA sheet remain unchanged.

Table 1 Details of stack materials used in this study.

Materials	Thickness (mm)	Density (kg/m^3)	Tensile modulus (GPa)	Yield strength (MPa)	Ultimate yield strength (MPa)	Nominal failure strain
AA1060-H24	1.0	2700	8.6	108	130	0.180
CFRP	0.5	1420	58	--	310	0.063
CFRP	1.0	1420	58	--	650	0.122
CFRP	1.5	1420	58	--	940	0.181

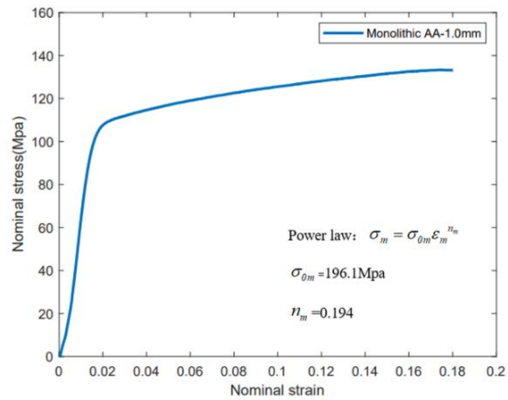

(a)

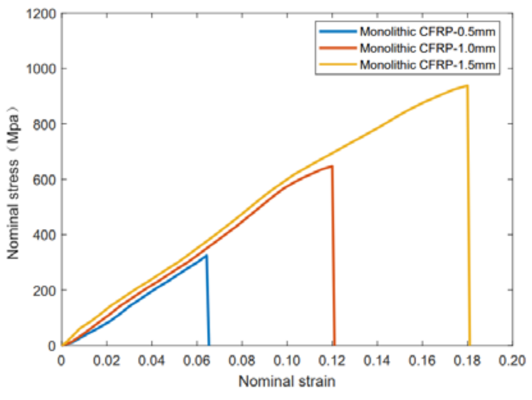

(b)

Fig.1 Tensile stress-strain curves of monolithic sheets: (a) AA sheet, (b) CFRP sheet

Experiments

All the tests were conducted on a four-axis vertical machining center (MIKRON® VCE 800 W Pro). Tungsten carbide hemispherical tools with different diameters (e.g. 5 mm, 10 mm and 15 mm) were used to deform AA/CFRP laminates. The tool was fixed not to rotate for all the tests. A circular steel clamping ring with an inner diameter of 50 mm was used to constrain the deformation boundary, which means that the maximum deformation area in our tests is a circular shape with a diameter of 50 mm. Before tests, the AA/CFRP stack sheet was clamped on the frame with the clamping ring and blank holders. During tests, the tool was numerically controlled by a Heidenhain iTNC530 controller which follows the specifically designed tool movements.

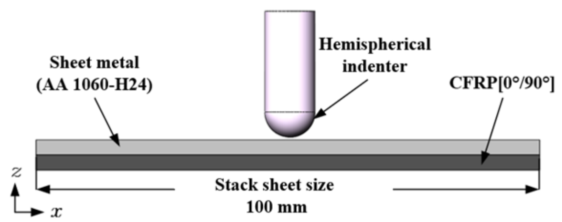

Fig.2 Schematic diagram of AA/CFRP stack sheet perforated by a hemispherical indenter

To capture the deformation dynamics, a dynamometer was used in this study, which has three channels to measure forces for the x, y and z directions (maximum ranges: x-5000 N, y-5000 N, z-10000 N) in the experiments. The dynamometer produces analog signals whose magnitude is directly proportional to the force. During the tests, analog signals transmitted from the dynamometer are first input into the NI 9237 Module with 1-slot cDAQ Chassis 9191, which provides a USB interface for four channels of 24-bit half/full-bridge analog input, and then connected to the laptop by Ethernet or 802.11 Wi-Fi in order to record the force signals using LabVIEW software. The details of the experimental setup with the dynamometer system are presented in Figure 3.

The quasi-static perforation experiments were carried out using the above-mentioned experimental apparatus. The indentation tests were stopped until the tool indenter had fully perforated all layers. In all quasi-static tests, no lubrication was used and the speed of the tool indenter was set to be 10 mm/min.

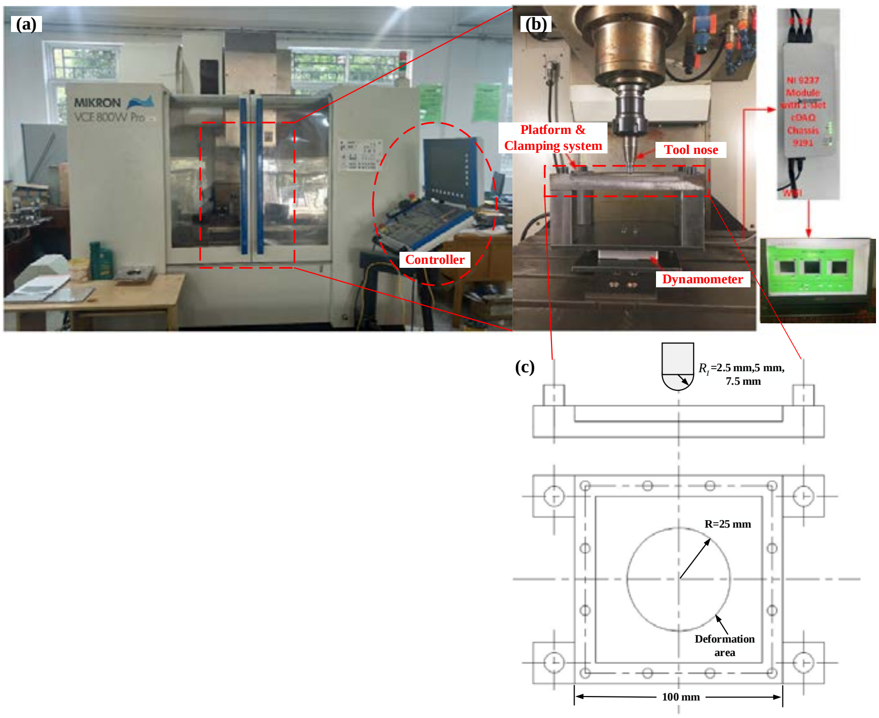

Fig.3 Experimental apparatus: (a) four-axis vertical machining center; (b) experimental setup with dynamometer system; (c) details of platform

RESULT

Quasi-static perforation performance of monolithic metallic and monolithic CFRP sheets

The general description of the quasi-static perforation responses of monolithic AA and monolithic CFRP sheets is presented in Fig.4 for tool indenter with three different sizes based on experimental data.

From Figure 4, we can see that the two stages can be identified in terms of quasi-static perforation responses. It is noted that Stage I is the phase in which a linear increase of perforation force versus displacement occurs. In addition, in this stage, micro-damage initiates and progresses until the macro penetration failure is witnessed, which corresponds to the peak force in the force-displacement curve. Stage II describes the deformation behavior that corresponds to the sharp load drop after the occurrence of macro material failure.

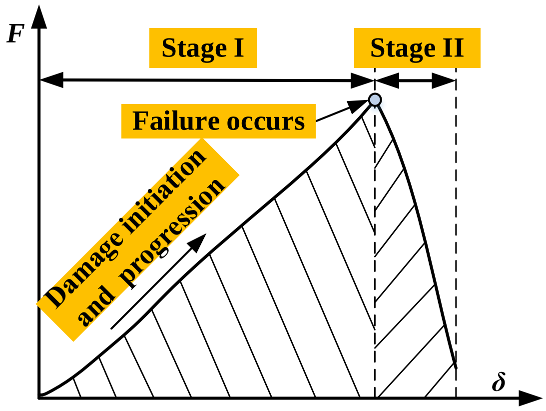

Fig.4 Illustration of the quasi-static perforation responses of monolithic AA and CFRP sheets based on experimental data.

Quasi-static perforation responses for different monolithic specimens and tool indenter diameters are provided and compared in Figure 5 and Table 2. Results show that a sheet loaded by the hemispherical-shape indenter with a diameter of 5 mm fails at the smallest displacement (both Stage I and Stage II), which also corresponds to the lowest level of peak force no matter what sheet materials (AA or CFRP) are. On the other side, a larger contact area between tool indenter and sheet induces larger peak penetration force, and so is the corresponding displacement at failure point (Stage I). Besides, an approximately linear increase can be identified in Figure 5 as the tool indenter diameter increases from 5 mm to 15 mm for both AA and CFRP specimens.

For an AA sheet, elastic and plastic bending is the main deformation mode during perforation with a hemispherical indenter before the peak failure point (Stage I). After that (Stage II), stretching mode dominates the deformation process. The material begins to be drawn out by the indenter, which can reach high levels of strain before it is failing. As noted in Figure 6, crack morphology shows that a circumferential crack first occurs at the tip of the tool nose (right after Stage I) and propagates as the penetration goes on (Stage II). At the same time, some minor radial cracks could be also witnessed. The detached material looks like a circular cap but its radius slightly less than that of the tool indenter. It is noting that the deformation in Stage I dissipates most of the energy compared to that in Stage II, as shown in Table 3. In addition, with the increasing of tool indenter diameter, a significant increase in the corresponding dissipation energy can be found, which means perforating a larger area of AA material needs more energy.

The deformation behavior of the CFRP sheet is very similar to that of the AA sheet. However, the onset of failure is advanced compared to the AA sheet. This is because the tensile strength of the CFRP sheet is smaller than that of the AA sheet. Besides, as the thickness of CFRP sheet varies, it shows little influence on the tool displacement in terms of the onset of failure in **Stage I**, as well as that in **Stage II.** On the other hand, the dissipated energy for penetrating a CFRP sheet is far smaller than that for penetrating the AA sheet of the same thickness.

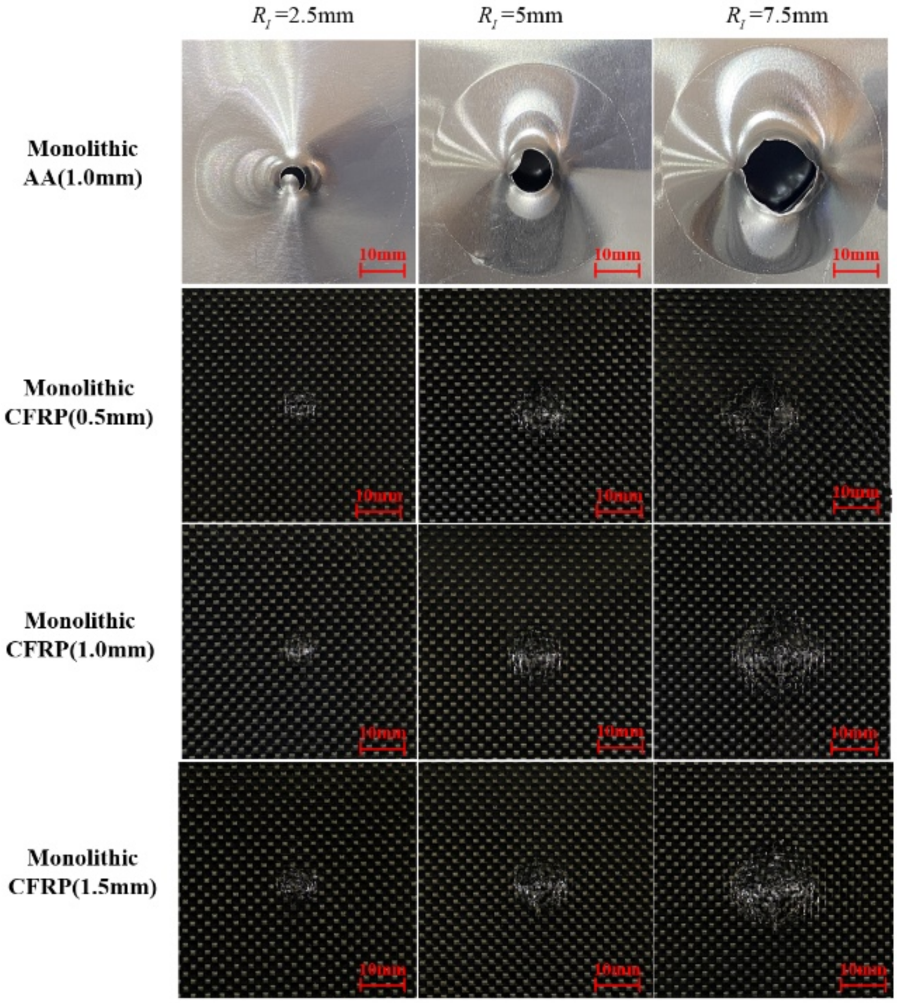

Fig.6 Failure morphology of monolithic AA and monolithic CFRP sheets under the quasi-static perforation with different tool indenter diameters.

Table 2. Comparison of quasi-static perforation responses for different specimen and tool nose diameters.

Specimen	Tool indenter diameters (mm)	Quasi-static perforation response		
		Peak force (N)	Displacement (mm, Stage I)	Displacement (mm, Stage II)
AA (1.0mm)	5 10 15	1199.07 1818.86 2640.48	6.69 7.37 8.62	2.21 4.01 8.09
CFRP (0.5mm)	5 10 15	166.30 395.96 664.59	3.05 3.48 5.54	3.21 5.20 6.10
CFRP (1.0mm)	5 10 15	223.55 606.78 972.50	4.77 4.52 4.97	2.67 5.32 9.72
CFRP (1.5mm)	5 10 15	611.19 972.58 1424.48	4.14 4.89 5.13	3.38 6.48 9.46

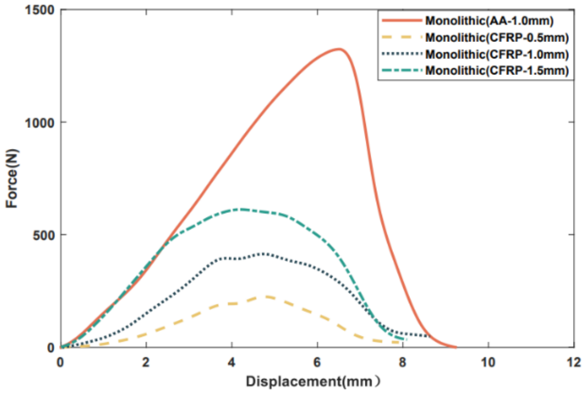

(a)

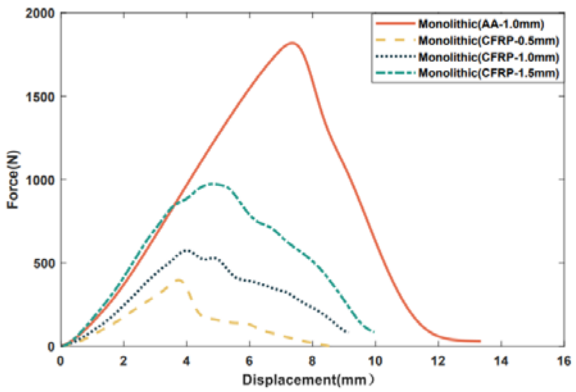

(b)

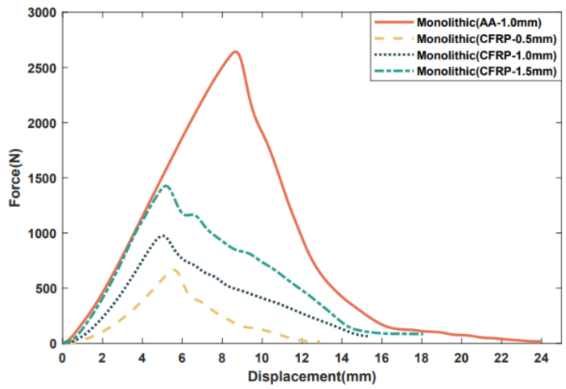

(c)

Fig.5 Quasi-static perforation response of CFRP and AA monolithic sheets with one thickness of AA sheet (1.0 mm), three thicknesses of CFRP (0.5 mm, 1.0 mm and 1.5 mm) and three different tool indenter sizes: (a) indenter diameter = 5 mm, (b) indenter diameter = 10 mm and (c) indenter diameter = 15 mm.

Effect of layer arrangements in AA/CFRP stack sheets

In this section, the effect of layer arrangements in the AA/CFRP stack sheets on the quasi-static perforation performance is analyzed. As described in Section 2.1, the proposed AA/CFRP laminated material is composed of an AA layer and a CFRP layer. The thickness of the AA layer is 1.0 mm. Three thicknesses (0.5 mm, 1.0 mm, and 1.5 mm) of CFRP layers were chosen to explore the deformation mechanism and to test the perforation resistance of hemispherical indenters with different sizes.

The quasi-static perforation responses are shown in Figure 7 for different tool indenter sizes. In each case, six main results are presented: stack sheet (CFRP-0.5 mm, back), stack sheet (CFRP-0.5 mm, front), stack sheet (CFRP-1.0 mm, back) stack sheet (CFRP-1.0 mm, front), stack sheet (CFRP-1.5 mm, back), and sheet stack (CFRP-1.5 mm, front).

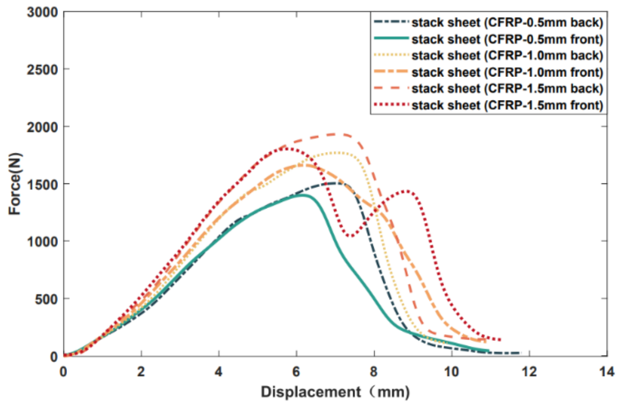

(a)

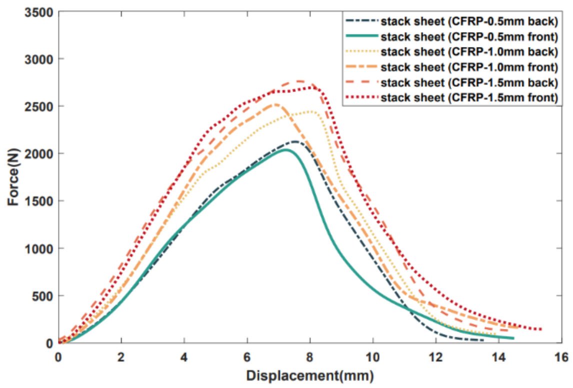

(b)

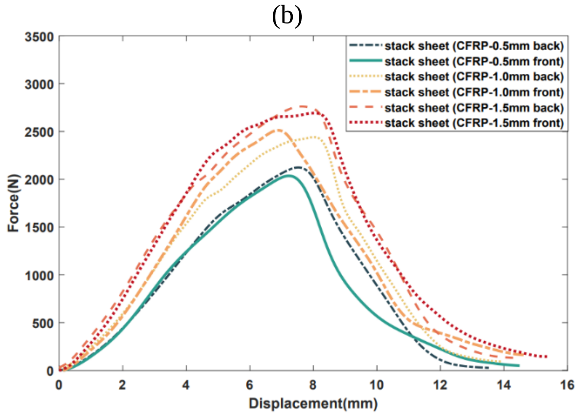

(c)

Fig.7 Quasi-static perforation responses of AA/CFRP stack sheets with three thicknesses of CFRP(0.5 mm and 1.0 mm and 1.5mm) for three different tool indenter sizes: (a) tool indenter diameter=5 mm, (b) tool indenter diameter=10 mm, (c) tool indenter diameter=15 mm. The label 'back' and 'front' denote the AA sheet facing the tool indenter and CFRP sheet facing the tool indenter, respectively.

CFRP sheet facing tool indenter

First, we consider the mechanical responses of CFRP/AA stack sheets with the CFRP layer facing the tool indenter, depicted by the green solid line (CFRP-0.5 mm), the orange dot-dashed line (CFRP-1.0 mm) and the red dot line (CFRP-1.5 mm). From the experimental results, it is noting that the failure of the metal (AA) layer can be advanced to some extent when the CFRP sheet is facing the tool. This phenomenon is observed regardless of the tool indenter diameter and the CFRP sheet thickness. This illustrates that the penetration-resistant characteristic is not obvious when placing the CFRP in front of the indenter. What is more, in Figure 8, a dishing deformation is observed first. Then, tensile tearing at the center of the sheet dominates the failure mode. This conclusion is in agreement with our previous findings in [20] (Liu and Chen et al., 2020).

AA sheet facing tool indenter

When the AA metal layer faces the tool indenter, the force response is approximately the superposition of the force of the AA and CFRP layers. During the perforation process, the AA layer fails in a very similar way compared with the monolithic metal plate, as shown in Figure 8. It means that there is no obvious effect on the deformation mode and fracture, and therefore no effect on the energy dissipation in **Stage I**. However, energy dissipation in **Stage II** can be influenced slightly as the CFRP layer is able to resist metal bending deformation. In addition, the AA metal layer could be postponed as the thickness of CFRP increases.

Table 3 Comparison of quasi-static perforation energies for different sheets and tool indenter diameters.

Specimen (Thickness: mm)	Tool indenter diameters (mm)	Quasi-static perforation energy (J)		
		Stage I	Stage II	Total
AA(1.0)	5 10 15	4.06 6.49 10.99	1.08 3.88 8.50	5.14 10.37 19.49
CFRP(0.5/1.0/1.5)	5 10 15	0.46/0.60/1.69 0.58/1.27/2.20 1.66/2.32/3.65	0.35/1.29/1.30 0.60/2.39/3.24 1.21/4.04/6.91	0.81/1.89/2.99 1.18/3.66/5.44 2.87/6.36/10.56
CFRP (0.5)/AA(1.0) stack sheets (*/^)	5 10 15	4.72/5.35 7.88/8.59 11.43/13.85	2.08/2.31 4.12 /4.40 10.92/10.77	6.80/7.66 12.00/12.99 22.35/24.62
CFRP (1.0)/AA(1.0) stack sheets(*/^)	5 10 15	4.70/6.90 8.38/12.08 13.79/16.72	5.00/2.19 8.00/4.15 16.17/13.32	9.70/9.09 16.38/16.23 29.96/30.04
CFRP (1.5)/AA(1.0) stack sheets (*/^)	5 10 15	5.30/6.04 12.18/12.10 20.00/18.60	5.60/3.20 7.87/7.38 12.10/12.75	10.91/9.24 20.05/19.48 32.10/31.35

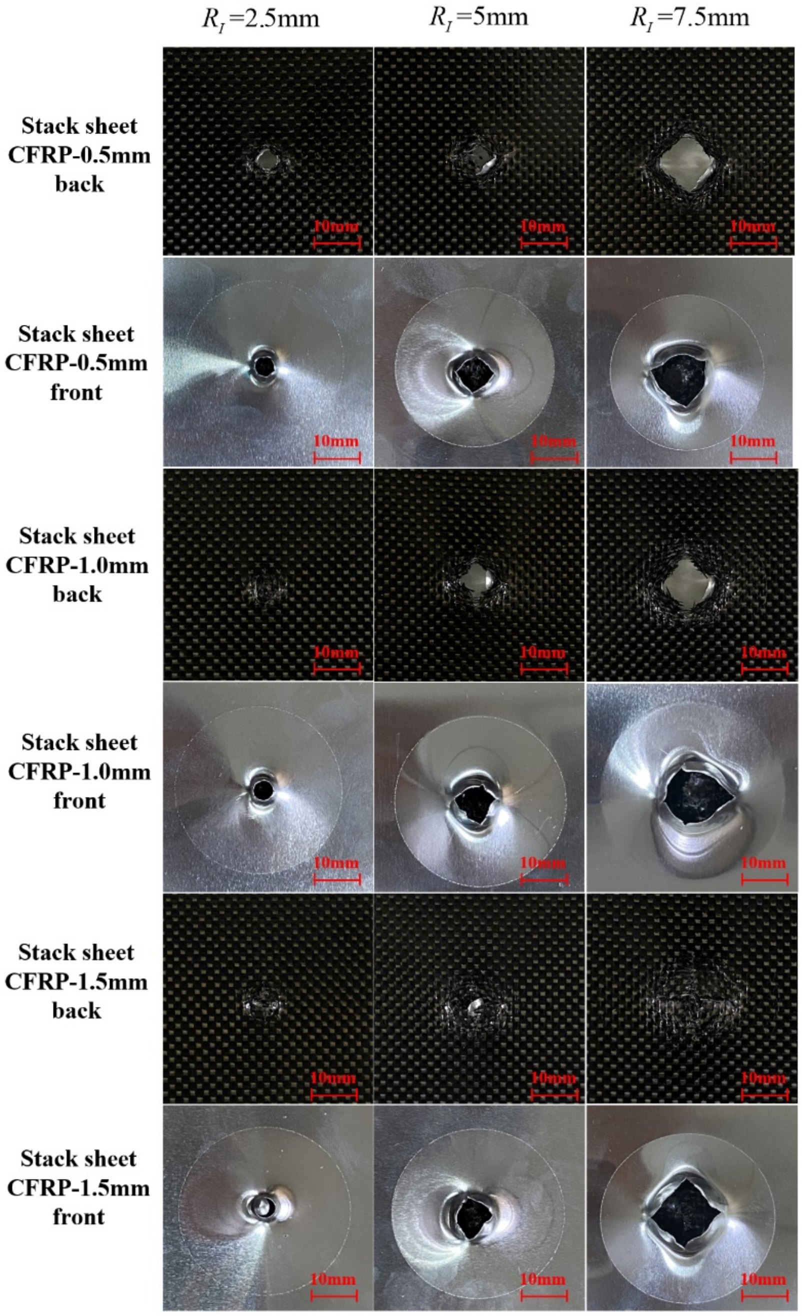

Fig.8 Failure morphology of AA/CFRP stack sheets under the quasi-static perforation with different tool indenter diameters when CFRP sheet facing or backing the tool indenter.

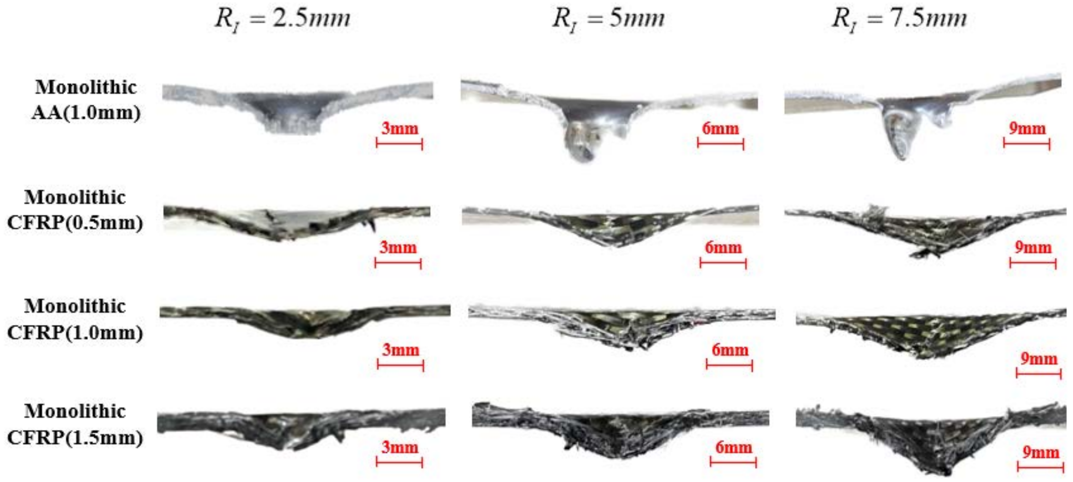

(a) Cross-sectional damage patterns of monolithic AA and monolithic CFRP sheets under quasi-static perforation with different tool indenter diameters.

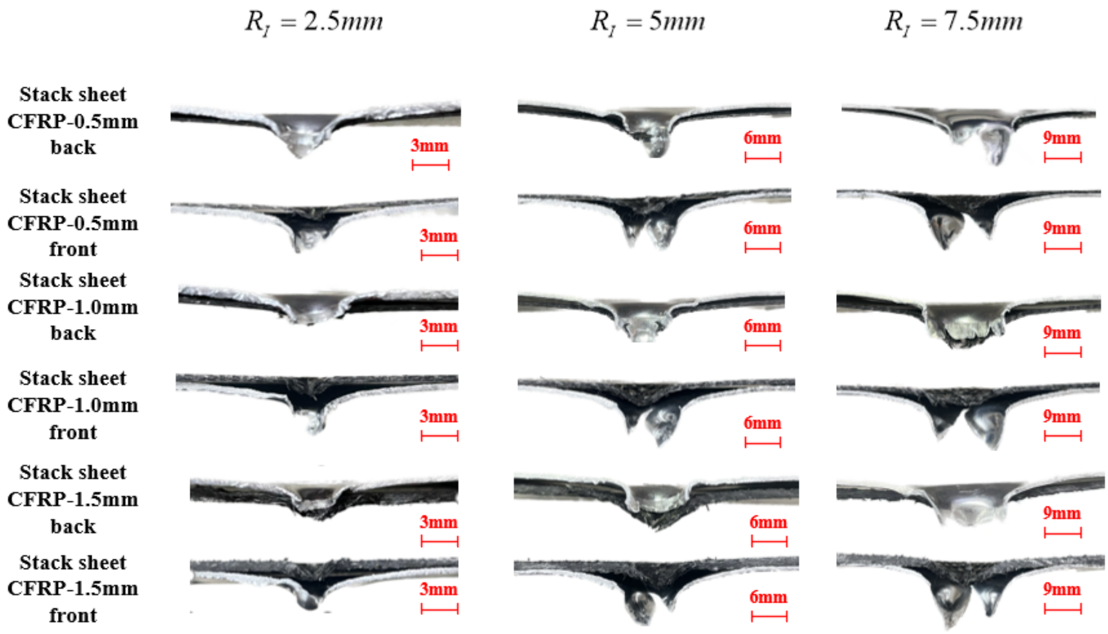

（b）Cross-sectional damage patterns of AA/CFRP stack sheets under the quasi-static perforation with different tool indenter diameters when CFRP sheet facing or backing the tool indenter.

Fig.9 Experimental cross-sectional damage patterns of monolithic and stack sheets under the quasi-static perforation with different tool indenter diameters.

Further, Figure 9 shows the experimental cross-sectional damage patterns of monolithic and stack sheets under the quasi-static perforation with different tool indenter diameters. From the cross-sectional results, we further demonstrate that the failure of the metal (AA) layer can be advanced to some extent when the CFRP sheet is facing the tool. A dishing deformation is observed first. Then, tensile tearing at the center of the sheet dominates the failure mode. On the other side, when the CFRP sheet is facing the tool, the CFRP layer is able to resist metal bending deformation. In addition, the AA metal layer could be postponed as the thickness of CFRP increases.

The damage pattern of AA metal layer under 5mm indenter diameter is a circular shape regardless of monolithic or stack sheets, while the damage pattern of AA metal layer in the other two diameter cases shows a petaloid shape. This is mainly because a smaller tool contact surface during perforation more easily experiences from elastic bending to a whole circumferential tensile tearing. By contrast, a larger tool contact surface leads to bi-axial even multi-axial tensile tearing. In addition, the damage pattern of CFRP sheets under three tool indenters shows an irregular shape due to the breakage of fiber and matrix, which is slightly different compared to the AA metal sheet.

Quasi-static perforation energy: analytical modeling versus experimental analysis

Energy absorption under perforation loading is an index to evaluate the perforation-tolerant performance of the proposed materials. It is obvious that the absorbed energy is equal to the area under the load-deflection curve up to the final failure position, as represented in Figure 5 and Figure 7, which can be computed based on the trapezoidal integral method. The quasi-static perforation energies for different material configurations and tool indenter diameters are concluded in Table 3.

Analytical prediction model for perforation energy

The perforation energy can be evaluated with analytical prediction models originally developed by Simonsen and Lauridsen (2000) for monolithic sheets and further modified by Mohagheghian et al. (2016) and Liu and Chen (2020) to deal with stack sheets. For monolithic metal sheet, the perforation energy $E_{p(m)}$ is predicted by

$$E_{p(m)} = \sigma_0 \pi R^3 \bar{m} \bar{R}_I \times \left\{ 0.318 \left(\bar{R}_I \right)^{0.607 - 0.387 \bar{R}_I + 1.2 \left(\bar{R}_I \right)^2} + 0.067 \left(n_m - 0.2 \right) \right\} \tag{1}$$

It is worth noting that in our study, the CFRP layer was not bonded to the metal plate, which is the same as in (Mohagheghian et al., 2016) and (Liu and Chen et al., 2020) where there was no bond between the metal and polymer layers.

For AA /CFRP stack sheets, the perforation energy $E_{p(l)}$ is given by

$$E_{p(l)} = \sigma_0 \pi R^3 \bar{t}_m \Phi \times \left\{ 0.318 \Phi^{0.607 - 0.387 \Phi + 1.2 \Phi^2} + 0.067 \left(n_m - 0.2 \right) \right\} \tag{2}$$

The parameters in the above models are illustrated as follows. First, the mass (per unit area) for a given stack sheet can be expressed as

$$\Phi = \bar{R}_I + \bar{m} \bar{\rho} - \bar{t}_m \bar{\rho} \tag{3}$$

$$m = \rho_m t_m + \rho_c t_c \tag{4}$$

where ρ_m and ρ_c are the densities of the AA and CFRP, respectively.

CFRP/metal stack sheets mass

$$\bar{m} = m / \left(\rho_m R \right) \tag{5}$$

Metal sheet thickness

$$\bar{t}_m = t_m / R \tag{6}$$

Tool indenter radius

$$\bar{R}_I = R_I / R \tag{7}$$

Density ratio

$$\bar{\rho} = \rho_m / \rho_c \tag{8}$$

For the case of a monolithic metal sheet, the tool radius is simply R_I. In contrast, for the case of the stack sheets in contact with the CFRP layer, the effective tool indenter radius $R_{I(e)}$ is assumed to be

$$R_{I(e)} = R_I + t_c \tag{9}$$

It is noted that in (9), the thinning of the CFRP is neglected, and can be considered as an upper bound for the effective radius, which is used in the derivation of the formula (2).

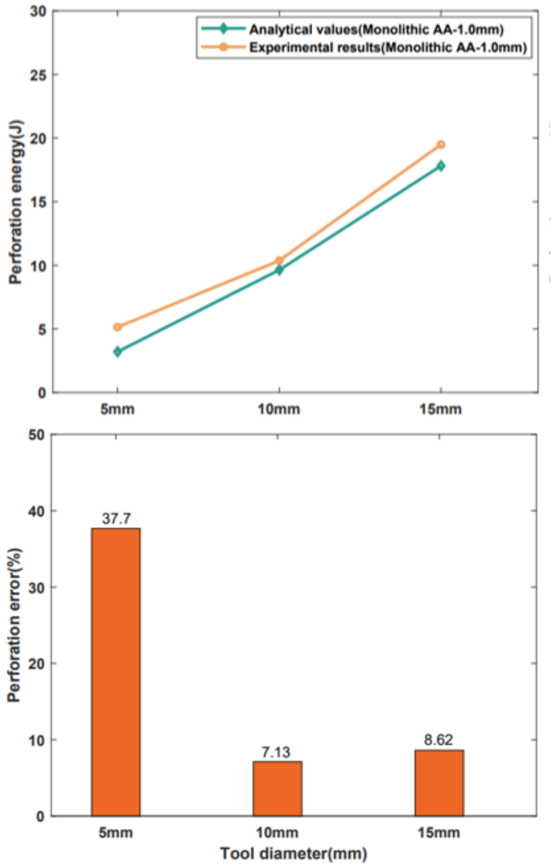

(a)

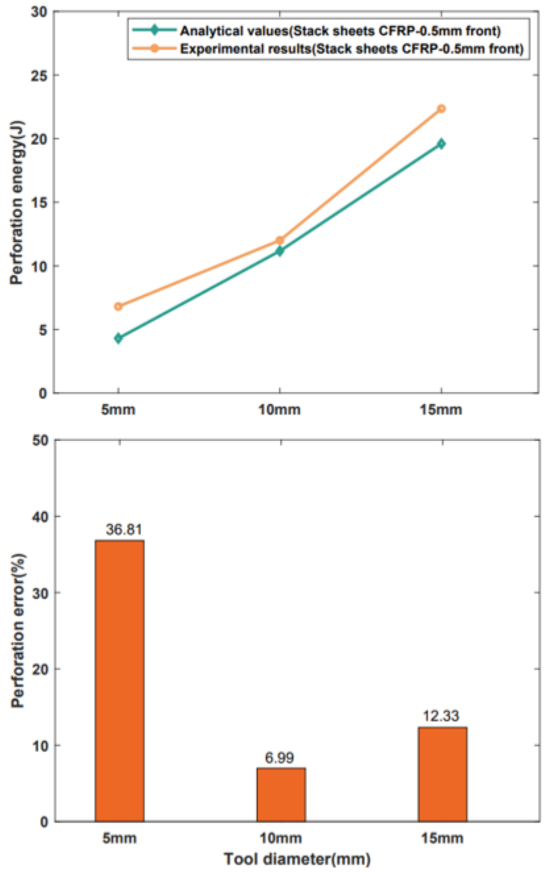

(b)

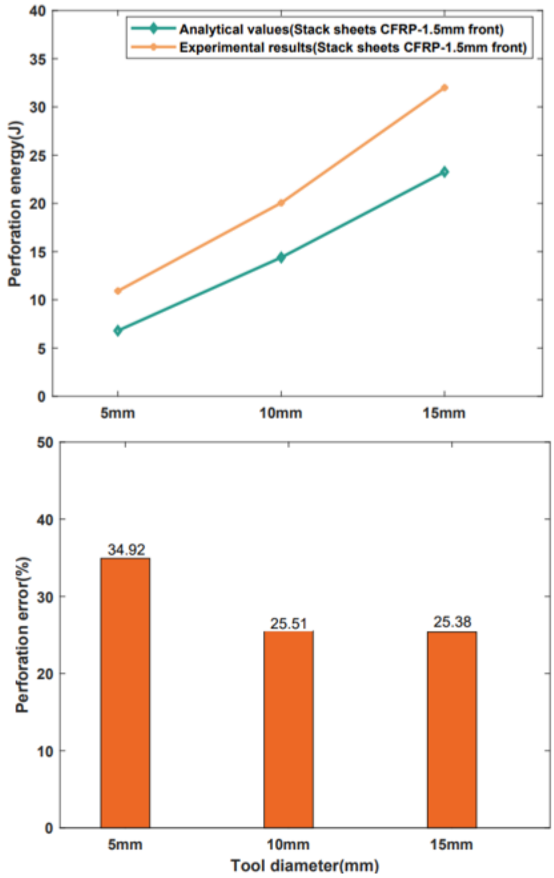

(d)

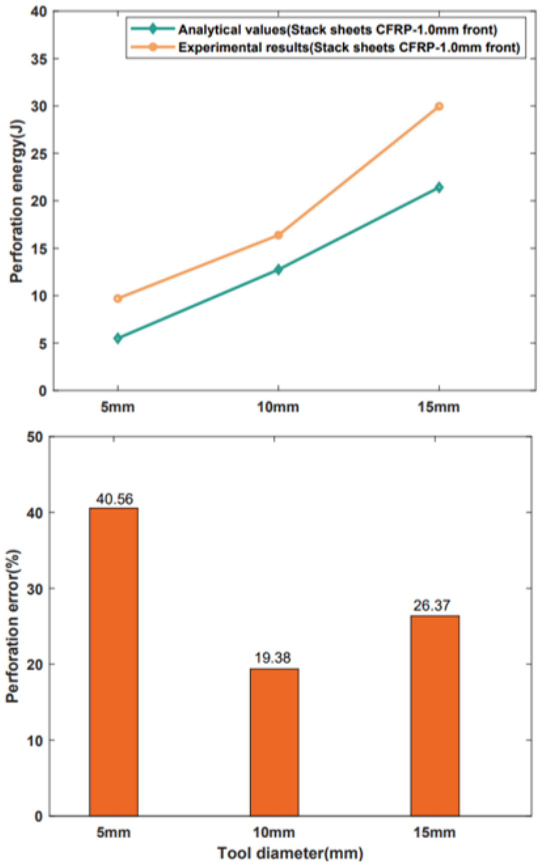

(c)

Fig.10 Comparison of predicted and experimental results of quasi-static perforation energy in the case of monolithic AA plate and AA/CFRP stack sheets with CFRP layer facing the tool indenter for three different tool diameters: (a) Monolithic AA-1.0 mm; (b) Stack sheet CFRP-0.5 mm; (c) Stack sheet CFRP-1.0 mm. (d) Stack sheet CFRP-1.5 mm.

Validation of analytical models

As discussed in (Mohagheghian et al., 2016) and (Liu and Chen et al., 2020), the formulas (1) and (2) are valid when the parameters are within the range of R/R_I =2~10 and n_m =0.1~0.3. In this study, R/R_I =3.3,5,10 and n_m =0.194 satisfy the parametric selection range.

As shown in Figure 10, the obtained formulas are able to correctly predict the trend of the quasi-static perforation energy. However, the analytical values are under-predicting the experimental results. This is because that in the experiments, the CFRP and AA layers could be clamped to the frame firmly as the deformation area is relatively small, thereby increasing the strength of the AA/CFRP stack sheets as a whole material. Besides, the perforation energy increases in an approximately linear manner with the increasing of tool indenter diameters in all cases. The predicted perforation error of 5 mm indentation head is significantly higher than the others. This is because the failure mode with 5 mm indentation head is the whole circumferential tensile tearing that needs relatively more perforation energy. While the failure mode of the other two cases is the bi-axial even multi-axial tensile tearing, less perforation energy is needed. This leads to that the calculation of predicted error of 5 mm indentation head is obviously higher than the others.

Conclusions

In this paper, we present a kind of AA/CFRP stack sheet materials. For such materials, the perforation behaviors and corresponding damage modes under different quasi-static loading conditions are investigated through analytical and experimental analyses. The mechanical performances, especially the perforation resistance, are explored considering the effects of tool indenter sizes, material layer arrangements and mechanical properties of each layer compared to the monolithic materials. In summary, the main contributions are as follows.

- For quasi-static perforation loads, the deformation and damage-resistant properties of the AA/CFRP stack sheets are very sensitive to the tool indenter sizes and arrangements of the material layers. If the CFRP layer faces the tool indenter, failure in the AA layer could be advanced slightly. This phenomenon is observed regardless of the tool indenter diameter and the CFRP sheet thickness. This illustrates that the penetration-resistant characteristic is not obvious when placing the CFRP in front of the indenter. In this case, a dishing deformation of the metal sheet is observed first, followed by tensile tearing.
- When the AA layer faces the tool indenter, the mechanical behavior of the stack sheet strongly depends on the failure mode of the metal plate. It is observed that the metal layer fails in a very similar way to the monolithic metal sheet. Nevertheless, the CFRP sheet was able to resist more bending deformation of the metal layer, thereby increasing energy dissipation. Furthermore, increasing the thickness of the CFRP sheet could postpone the fracture of the metal layer.
- An analytical model is proposed to predict the perforation energy of AA/CFRP stack sheet materials with CFRP layer facing the tool indenter. The developed model correctly predicts the trend of the quasi-static perforation energy, but obtains a prediction that is smaller compared to the experimental results. This is mainly due to the fact that the CFRP and AA layers could be clamped to the frame firmly as the deformation area is relatively small, thereby increasing the strength of the AA/CFRP stack sheets as a whole material. Furthermore, it is concluded that the perforation energy increases in an approximately linear manner as the tool indenter radius increases in all investigated cases.

Acknowledgments

This work is supported by the Open Project Program of Shandong Marine Aerospace Equipment Technological Innovation Center, Ludong University (Grant No. MAETIC2021-02).

References

Anbazhagan, S., Manikandan, P., Chai, G.B. and Joshi, S.C., “Quasi-static indentation characteristics of sandwich composites with hybrid facesheets: Experimental and numerical approach.”Journal of Sandwich Structures & Materials, Vol.24, No.1, pp.294-320 (2022).

Chen, C. H., Zhu, X., Hou, H. L. and Tian, X. B., “A new analytical model for the low-velocity perforation of thin steel plates by hemispherical-nosed projectiles,” Defence technology, Vol.13, No.5, pp.7-17 (2007)

Chow, Z.P., Ahmad, Z., Wong, K.J. and Abdullah, S.S., “Experimental and numerical analyses of temperature effect on glare panels under quasi-static perforation.” Composite Structures, Vol.275, pp.114434 (2021).

Garrido, M., Teixeira, R., Correia, J.R. and Sutherland, L.S., “Quasi-static indentation and impact in glass-fibre reinforced polymer sandwich panels for civil and ocean engineering applications,” Journal of Sandwich Structures & Materials, Vol.23, No.1,pp.194-221 (2021).

Javanshour, F., Prapavesis, A., Prnnen, T., Orell, O., Belone, M.L., Layek, R. K. and Sarlin, E., “Modulating impact resistance of flax epoxy composites with thermoplastic interfacial toughening,” Composites Part A: Applied Science and Manufacturing, Vol-150, pp.106628 (2021).

Kuo, C., Li, Z, and Wang, C., “Multi-objective optimisation in vibration-assisted drilling of CFRP/Al stacks,” Composite Structures, Vol.173,pp.196–209 (2017).

Linforth, S., Ngo, T., Tran, P., Ruan, D. and Odish, R., “Investigation of the auxetic oval structure for energy absorption through quasi-static and dynamic experiments,” International Journal of Impact Engineering, Vol-147, pp.103741 (2021).

Liu, Z. and Chen, H., “Deformation mechanism and failure-tolerant characteristics of polymer-coated sheet metal laminates subjected to different loading conditions,” Journal of

Materials Research and Technology, Vol.9, No.3, pp.3907-3923 (2020).

Li, X., Ma, X., Li, S., Guo, Y., Shim, V.P.W.and Hao, X., "Deformation and failure of a novel fiber-metal hybrid lamina composite under quasi-static and impact loading," Composites Science and Technology, Vol.216, pp.109067 (2021).

Luo, B., Li, Y., Zhang, K., Cheng, H. and Liu, S., "A novel prediction model for thrust force and torque in drilling interface region of CFRP/Ti stacks," International Journal of Advanced Manufacturing Technology, Vol.81, No.9, pp.1497-1508 (2015).

Mohagheghian, I., McShane, G.J. and Stronge, W.J., "Impact perforation of monolithic polyethylene plates: Projectile nose shape dependence," International Journal of impact engineering, Vol.80, pp.162-176 (2015).

Mohagheghian, I., Stronge, W.J. and McShane, G.J., "Predicting indenter nose shape sensitivity for quasi-static perforation of thin metallic plates," European Journal of Mechanics-A/Solids, Vol.61, pp.134-150 (2017a).

Mohagheghian, I., McShane, G.J. and Stronge, W.J. "Quasi-static and impact perforation of polymer-metal bi-layer plates by a blunt indenter," Thin-walled structures, Vol.117, pp.35-48 (2017b).

Mohagheghian, I., McShane, G.J. and Stronge, W.J., "Impact perforation of polymer–metal laminates: Projectile nose shape sensitivity," International Journal of solids and structures, Vol.88, pp.337-353 (2016).

Schwab, M., Todt, M., Wolfahrt, M. and Pettermann, H. E.,"Failure mechanism based modelling of impact on fabric reinforced composite laminates based on shell elements," Composites Science and Technology, Vol.128, pp.131-137 (2016).

Simonsen, B. C. and Lauridsen, L. P., "Energy absorption and ductile failure in metal sheets under lateral indentation by a sphere," International Journal of Impact Engineerin, Vol.24, No.10, pp.1017-1039 (2000).

Smith, W.F., "Principles of materials science and engineering," pp.699-724 (1990)

Wierzbicki, T., "Petalling of plates under explosive and impact loading," International Journal of Impact Engineering, Vol.22, pp.935-954 (1999).

Xia, R.S. and Mahdavian, S.M., "Experimental studies of step drills and establishment of empirical equations for the drilling process," International Journal of Machine Tools & Manufacture, Vol.45, No.2, pp.235-240 (2005)

Xu, Z.W., Guan, Z.W. and Cantwell, W.J., "An experimental study of scaling effects in the perforation resistance of woven CFRP laminates," Composite Structures, Vol.181, pp.285-293 (2017).

Yeganeh, E.M., Liaghat, G.H. and Pol, M.H., "Laminate composites behavior under quasi-static and high velocity perforation," Steel and Composite Structures, Vol.22, No.4, pp.777-796 (2016).

Yuan, K., Liu, K., Wang, Z. and Yang, M., "An investigation on the perforation resistance of laminated CFRP beam and square plate," International Journal of Impact Engineering, Vol.157, pp.103967 (2021).

Yu, B., Deshpande, V. S. and Fleck, N.A., "Perforation of aluminium alloy-CFRP bilayer plates under quasi-static and impact loading," International Journal of Impact Engineering, Vol-121, pp.106-118 (2018).

Yu, B., Karthikeyan, K., Deshpande, V.S. and Fleck, N.A., "Perforation resistance of CFRP beams to quasi-static and ballistic loading: The role of matrix strength," International Journal of Impact Engineering, Vol.108, pp.389-401 (2017).

Zitoune, R., Krishnaraj, V., Almabouacif, B. S., Collombet, F., Sima, M. and Jolin, A.,"Influence of machining parameters and new nano-coated tool on drilling performance of CFRP/Aluminium sandwich," Composites Part B: Engineering, Vol.43, pp.1480-1488 (2012).

Zitoune, R., Krishnaraj, V. and Collombet, F.,"Study of drilling of composite material and aluminium stack," Composite Structures, Vol.92, No.9, pp.1246-1255 (2010).

NOMENCLATURE

R: Radius of deformation area

R_I: Tool indenter radius

σ_{0m}: Strength coefficients of metal sheet

n_m: Strain-hardening exponents of metal sheet

t_m: Thicknesses of the metal and CFRP

ρ_m: Densities of the metal and CFRP

$\bar{m}$: Dimensionless parameter of CFRP/metal stack sheet mass

$\bar{t}_m$: Dimensionless parameter of metal sheet thickness

$\bar{R}_I$: Dimensionless parameter of tool indenter radius

$\bar{\rho}$:Dimensionless parameter of density

$R_{I(e)}$: Effective tool indenter radius

$E_{p(m)}$: Perforation energy of monolithic metal sheet

$E_{p(l)}$: Perforation energy of AA/CFRP stack sheet